Isomerizations of Bicyclo[2.1.0]pent-2-ene and Tricyclo[2.1.0.0^{2,5}]pentane into Cyclopenta-1,3-diene: A Computational Study by DFT and High-Level ab Initio Methods

İlker Özkan,* Armağan Kinal, and Metin Balci

Department of Chemistry, Middle East Technical University, 06531 Ankara, Turkey

Received: September 18, 2003; In Final Form: November 18, 2003

The thermal isomerizations of bicyclopentene (**bcp**) and tricyclopentane (**tcp**) into cyclopentadiene (**cp**) are investigated by a combination of DFT, CASSCF, CASSCF-MP2, and CR-CCSD(T) methods. Coupled-clusters and B3LYP methods predicted the reaction enthalpies excellently whereas the MCSCF method worked well only when dynamic correlation energy was taken into account. Both processes are concerted, and the reaction paths pass through transition states with high biradical character. Measures of biradical character in DFT and ab initio methods are discussed. The activation enthalpy in the rearrangement of **bcp** into **cp** was predicted by the CR-CCSD(T) method to be 25.5 kcal/mol, in good agreement with experiment. The UB3LYP functional also performed well in this case despite the high spin contamination that was present in the singlet biradicaloid transition state. The reaction enthalpy for the conversion of **tcp** into **cp** was predicted to be −63.7 kcal/mol. The transition state involved in the isomerization of **tcp** was found to be nearly degenerate with the triplet state causing less certainty in the estimated activation enthalpy of 48.3 kcal/mol.

Introduction

Bicyclo[2.1.0]pent-2-ene (**bcp**), first prepared in 1966 by Brauman, Ellis, and van Tamelen,[1a] is a strained, small-ring hydrocarbon of unusual structure. It was obtained from the photolysis of cyclopentadiene (**cp**) by a procedure that was subsequently refined by Baldwin's group[2] so that it could be secured in quantities sufficient for synthetic utilization and other experimental work. That the photolysis mixture also contained tricyclo[2.1.0.0^{2,5}]pentane (**tcp**), another photoproduct of cyclopentadiene, was later discovered by Andrews and Baldwin[2d] in 1977. The proportions of **cp**:**bcp**:**tcp** in the photolysis mixture were approximately 14:7:1. Whether cyclopentadiene or bicyclopentene is the immediate precursor of tricyclopentane was not established.

The main interest in **bcp** stems from its facile thermal conversion back to **cp**. Brauman and Golden[1b,c] investigated the kinetics of this rearrangement at temperatures between 26.0 and 108.4 °C and reported log $k(s^{-1}) = [(14.2 \pm 0.2) - (26.9 \pm 0.3)]/2.303RT$. They assumed that the reaction involved bridgehead bond cleavage in a disrotatory sense, a hypothesis violating the Woodward−Hoffmann[3] (W−H) rules of electrocyclic reactions, according to which the allowed process is the conrotatory rearrangement as in the conversion of cyclobutene to butadiene. There was a long debate lasting a decade about the reaction mode followed in the isomerization.[2,4,5] Recognizing the presence of steric constraints, researchers experimentally tested alternate W−H allowed pathways (e.g., hydrogen shift). Finally, ^{13}C labeling experiments carried out in 1977 by Andrews and Baldwin[2e] ended the controversy over the reaction mechanism in favor of the disrotatory, disallowed biradical process (Scheme 1). Thus, the isomerization of **bcp** constitutes a counterexample to the W−H rules. The molecular structure of **bcp** has been determined by its microwave spectrum.[2c] The experimental reaction enthalpy of **bcp** to **cp** conversion is also known,[6] −47.8 ± 0.5 kcal/mol at 25 °C.

SCHEME 1

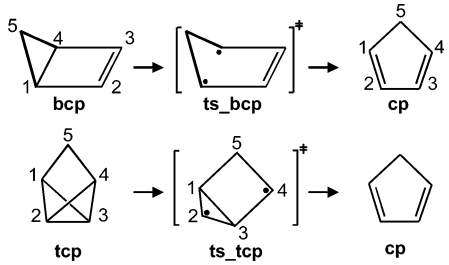

To our knowledge, only limited computational studies of the ring opening of **bcp** into **cp** have previously been made. Independent MINDO/3 calculations gave results at variance with each other.[7,8] Skancke, Yamashita, and Morokuma[9] (SYM) reported ab initio calculations on the reaction and activation energies of this reaction as part of their studies on the walk rearrangements of **bcp**. They obtained good agreement with experiment using the (U)MP4/6-31G(d)//(U)HF/3-21G methodology. The transition structure (TS) in the ring-opening process has a high degree of biradical (multireference) character as have the TSs involved in the walk rearrangements. In connection with the latter TSs, SYM's use of spin-contaminated UHF wave functions for the description of biradical states was criticized by Jensen,[10] who concluded that UHF-based methods give deviating results, and the MCSCF method is required to treat both closed-shell and biradical states on equal footing. The results obtained by SYM for the ring opening in **bcp** might thus be fortuitous.

Both the semiempirical calculations and SYM's work considered only the potential energy minima **bcp** and **cp** and the saddle **ts_bcp** structures. The complete reaction path from **bcp** to **cp** has never been followed. This is important because it has been suggested that forbidden pericyclic reactions cannot take

* Corresponding author. E-mail: ilker@metu.edu.tr. Tel: (+90)-3122105143. Fax: (+90)3122101280.

10.1021/jp036792b CCC: $27.50
Published on Web 12/23/2003

place in a concerted manner (i.e., the reaction path must pass through intermediates[1c,7]).

There have been several experimental studies of the thermal rearrangements of **tcp** and its derivatives.[11−18] Unfortunately, no experimental reaction parameters are available for the ring opening of this molecule. We are not aware of any high-level computational investigation of the rearrangement process in **tcp**. From a theoretical point of view, ring opening in **tcp** is a more challenging task than that in bcp because the former process involves the homolytic cleavage of two σ bonds whereas the latter has only one bond broken. The TS(s) and any intermediates if they exist are expected to have a substantial amount of biradical character. Furthermore, **tcp** has C_{2v} symmetry, having four equivalent C−C σ bonds of which two are to be broken during the reaction. Even though four electrons are actually involved in the process, the presence of four equivalent bonds complicates the theoretical analysis.

The present study is particularly aimed at determining the characteristic features of that portion of the potential energy surface concerning the three closed-shell species **cp**, **bcp**, and **tcp** in Scheme 1. Because of the presence of biradical TSs on the reaction paths, it is not clear at the outset whether a single method (e.g., DFT or MCSCF) is capable of handling all of the five species involved with comparable accuracy. To cross-check the validity of the results predicted by different methods and assess the possible errors, we here report calculations at a number of different levels of theory. Specifically, by combining the predictions of DFT, CASSCF, multireference Moller−Plesset perturbation theory (CASSCF-MP2), and coupled-clusters (CC) methods, we hope to obtain reliable values for the reaction parameters.

Computational Methods

Pople's 6-31G(d) split-valence basis set[19,20] was used throughout. DFT calculations employed the (U)B3LYP[21,22] and (U)BPW91[23] functionals as implemented in the Gaussian 98 program.[24] The former functional is generally regarded as an effective and economical means for comparing the structures and energetics in both concerted and stepwise rearrangement processes.[25] However, its validity in cases that involve species with a relatively high degree of biradical character has recently been questioned by Staroverov and Davidson[26] in connection with the extensively studied Cope rearrangement.[27] They concluded that the tight diyl intermediate predicted by the spin-contaminated UB3LYP method in the Cope rearrangement was probably spurious and conjectured that the problem might be due to the contribution of the UHF exchange in the B3-hybrid exchange functionals. Staroverov and Davidson suggest that the pure (U)BPW91 functional provides a more reliable method in such cases.

CASSCF calculations were carried out mainly by the GAMESS program.[28] Two different sizes of the active spaces were used, denoted as CAS44 and CAS88. The CAS44 consisted of four electrons in four orbitals, (4e, 4o), yielding 20 configuration state functions (CSF) when symmetry is not used. The active orbitals were the four π MOs in the case of the planar cyclopentadiene structure. The orbitals at all other points on the PES were in accord with those at the **cp** structure. Complete intrinsic reaction coordinate[29] (IRC) calculations were carried out to make sure that the correct active space was employed at less obvious structures such as **tcp** and the TS connecting it to **cp**. The GAMESS program was used for this purpose. The active orbitals at the **tcp** structure were two sets of (σ, σ*) orbitals corresponding to two of the four equivalent C−C bonds in this molecule. It is possible to select the two bonds either as that pair related by a C_2 rotation or as another pair related by the σ_v plane. The two selections distort the C_{2v} symmetry of **tcp** into C_2 and C_s symmetries, respectively. The CAS44 calculations reported in this paper refer to the former choice. To maintain the C_{2v} symmetry of **tcp**, it is necessary to take all four equivalent bonds into account, giving the (8e, 8o) CAS88 for a total of 1764 CSFs. As in the CAS44 case, full IRC calculations at the CAS88 level were performed to verify the continuous deformation of CAS at all points on the PES explored in this work.

Even the computationally demanding CAS88 method recovers only a small portion of the correlation energy (called the "static correlation"). To handle the dynamic correlation, we used the single-state multireference Moller−Plesset second-order perturbation theory (MP2) of Hirao and Nakano,[30] as implemented in the GAMESS program. The MP2 calculations with the CASSCF reference at CASSCF/6-31G(d) geometries are denoted by CAS44-MP2 and CAS88-MP2 for the two active spaces, respectively.

All force constant (Hessian) computations in both the DFT and CASSCF methodologies were carried out analytically using the Gaussian 98 program.[31] All stationary structures reported in this work were fully optimized at the (U)B3LYP, (U)BPW91, CAS44, and CAS88 levels. Transition structures were identified by the occurrence of a single imaginary vibrational frequency at the stationary geometries (minima have none).

To assess the amount of correlation energy recovered by DFT and CASSCF-MP2 methods at different points on the PES and hence to decide whether the approximate PESs generated by various methods are parallel to the exact PES, we need reliable reference energies against which we may compare the predictions of these methods. For this purpose, we employed the completely renormalized (CR) coupled-cluster theory of Piecuch et al. with single and double excitations and noniterative inclusion of triples.[32] This method, denoted by CR-CCSD(T), is also implemented in the GAMESS program.[33] Despite the fact that it is a single-reference method based on the closed-shell RHF determinant, it appears to yield excellent results even for biradical structures that normally require a multireference treatment.[34]

The correlation energy of species i recovered by a given method m is defined as the difference in the calculated energy from that using the RHF method, $E_{\mathrm{corr},i}(m) = E_i(m) - E_i(\mathrm{RHF})$. This definition will be used below to compare the performance of the ab initio methods. To include the DFT methods in the comparison, we choose a reference molecule and define a relative correlation energy by $\Delta E_{\mathrm{corr},i}(m) = E_{\mathrm{corr},i}(m) - E_{\mathrm{corr,ref}}(m)$. The reference used in our calculations was the cyclopentadiene molecule.

A biradical[35] (or diradical) is a molecule in which the unpaired electrons are localized at atomic centers separated by a relatively long distance. The two spins are only weakly coupled with the consequence that the singlet and triplet states of the system are nearly degenerate. Thus, the singlet−triplet (S−T) energy gap or $\langle S^2 \rangle$ value obtained by a spin-unrestricted method may be used as qualitative measures[36] of biradical character in a molecule. As the S−T gap decreases, the molecule acquires more biradical character, and $\langle S^2 \rangle$ calculated by UHF or UDFT increases. For the ab initio methods, more quantitative measures are available in the literature. Jensen[10] proposed a biradical index, $\mathrm{br} = 2 - n_h$, where n_h is the occupation number of the natural orbital corresponding to the HOMO. Staroverov and Davidson and others[37] suggested the use of what they called

TABLE 1: Electronic[a] and Zero-Point Vibrational[b] Energies (kcal/mol) of Various Species Relative to cp Calculated by Different Methods Using the 6-31G(d) Basis Set

	cp	bcp	tcp	ts_bcp	ts_tcp
(U)B3LYP[c]	−194.101058 (58.29)	48.12 (−0.43)	64.47 (−0.62)	73.95 (−2.96)	106.63 (−3.26)
(U)BPW91[d]	−194.071896 (56.77)	44.54 (−0.41)	58.18 (−0.57)	72.04 (−3.01)	102.75 (−3.16)
RHF[c]	−192.790176	50.65	66.63	95.49	145.37
CR-CCSD(T)[c]	−193.486405	46.95	64.39	74.69	115.19
CCSD(T)[c]	−193.494549	46.99	64.77	72.05	110.04
CAS44[e]	−192.846625 (61.30)	55.02 (0.02)	78.95 (0.32)	70.31 (−2.04)	114.98 (−1.99)
CAS44-MP2[e]	−193.433949	50.18	71.85	72.25	113.75
CAS88[f]	−192.899439 (61.26)	58.66 (−0.43)	79.90 (−0.20)	77.32 (−2.59)	121.01 (−2.41)
CAS88-MP2[f]	−193.426281	47.32	67.32	69.52	109.89
(U)B3LYP[g]	−194.153720 (57.84)	49.35 (−0.51)	66.47 (−0.67)	74.72 (−3.02)	108.19 (−3.40)
CCSD(T)[g]	−193.608951	46.04	63.23	70.48	108.96

[a] Electronic energies for the reference **cp** molecule are in hartrees. [b] ZPVEs in kcal/mol are shown in parentheses. ZPVEs of species other than **cp** are relative to that in **cp**. [c] Calculated at the (U)B3LYP optimized geometries. [d] Calculated at the (U)BPW91 optimized geometries. [e] Calculated at the CAS44 optimized geometries. [f] Calculated at the CAS88 optimized geometries. [g] 6-311G(d,p) basis set.

the "density of effectively unpaired electrons" as a probe of the biradical character. A Mulliken population analysis of this density gives effective numbers of unpaired electrons associated with each atom. The latter coincide with Mayer's free valence[38] in the case of singlet states.[37c] The free valences were calculated at the CAS88 level by the HONDO[39] program.

Results and Discussion

Reaction and Activation Energies. Density functional theory and CASSCF calculations agreed on the fact that both processes occur in a concerted manner as verified by following the complete IRCs (i.e., no intermediates were present along the reaction pathways). The main geometrical parameters[41] of the five stationary species (three minima and two TSs) optimized at the (U)B3LYP and CAS88 levels employing the 6-31G(d) basis set are shown in Figure 1. The electronic and zero-point vibrational energies (ZPVE) of all species calculated by different methods are conveniently summarized in Table 1. Coupled-clusters values in Table 1 refer to single-point calculations at the (U)B3LYP optimized geometries. Similarly, CAS44-MP2 and CAS88-MP2 calculations were carried out at the CAS44 and CAS88 optimized structures, respectively. To address the basis set effects, the structures of all five species were reoptimized at the (U)B3LYP level using the 6-311G(d,p)[40] basis set. The new geometries[41] were virtually identical to those at the (U)B3LYP/6-31G(d) level. We also computed CCSD(T) energies employing the 6-311G(d,p) basis set. The maximum difference between CCSD(T)/6-31G(d) and CCSD(T)/6-311G-(d,p) relative energies was 1.5 kcal/mol. It appears that basis set effects are rather minor for the species considered in this work. The B3LYP and CCSD(T) results with the 6-311G(d,p) basis are given in the last two rows of Table 1.

The three molecules **cp**, **bcp**, and **tcp** are considered first. Geometries of these species predicted by the DFT and CASSCF methods were in satisfactory agreement with each other as assessed by doing CC calculations. For each species, CR-CCSD-(T) energies of the structures optimized by DFT and CASSCF methods were the same within 1 kcal/mol. In assessing the relative energies predicted by a given method, we will use the highly accurate CR-CCSD(T) values as our reference energies. It is seen from Table 1 that the B3LYP functional performs excellently. The nonhybrid BPW91 functional is not as good, giving the energies of **bcp** and **tcp** relative to **cp** by 2.4 and 6.2 kcal/mol, respectively, too low. We note that in these closed-shell species both functionals were stable toward spin-symmetry breaking (i.e., energies could not be lowered by relaxing the spin restriction and hence $\langle S^2 \rangle = 0$). Both the CAS44 and the extensive CAS88 methods placed the energies of **bcp** and **tcp** too high relative to that of **cp**, differing from CC values by 8.1−11.7 and 15.5 kcal/mol in **bcp** and **tcp**, respectively. It is interesting that the much more flexible CAS88 is worse than CAS44 in the case of **bcp**, a fact clearly indicating that the inclusion of dynamical correlation is much more important than enlarging the CAS. Indeed, taking the dynamic correlation into account by the CASSCF-MP2 method brings both CASSCF energies within a few kcal/mol of the CC values, with CAS88-

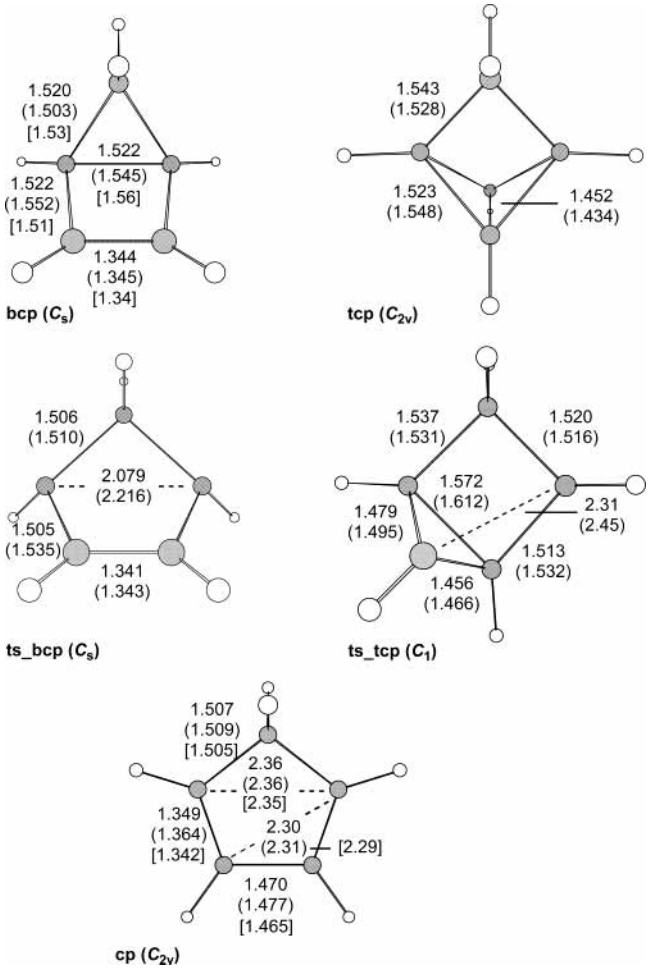

Figure 1. Selected interatomic distances (Å) and point groups for species[41] shown in Scheme 1. The uppermost values refer to the UB3LYP geometry. The corresponding CAS88 values are indicated inside parentheses, and the experimental values (when available) are shown inside square brackets (ref 2c for **bcp** and ref 42 for **cp**).

TABLE 2: Correlation Energies of Various Species at (U)B3LYP/6-3G(d) Optimized Structures as Predicted by the ab Initio Methods[a]

	CAS44 (%)	CAS44-MP2 (%)	CAS88 (%)	CAS88-MP2 (%)	CR-CCSD(T) kcal/mol
cp	8.0	92.5	15.5	91.4	−436.89
bcp	6.9	91.8	13.5	91.4	−440.59
tcp	5.1	91.0	12.3	90.8	−439.14
ts_bcp	13.2	94.2	18.9	93.7	−457.70
ts_tcp	14.3	94.1	20.1	93.7	−467.07
average	9.5	92.7	16.1	92.2	−448.28

[a] CASSCF and CASSCF-MP2 values are given as percentages of those in the CR-CCSD(T) column.

MP2 working somewhat better. It will be noted from Table 1 that the RHF energies of the stable species calculated at the B3LYP geometries are within 3.7 kcal/mol of the CC values, an accuracy approaching that of CAS88-MP2. Evidently, the total correlation energies in **cp**, **bcp**, and **tcp** must be nearly the same. In light of this fact, the poor performance of CASSCF can be understood. The fraction of correlation energy recovered by CASSCF is significantly dependent on the molecule considered (i.e., the CASSCF method does not recover the same fraction of the correlation energy at different points on the PES).

Table 2 shows the total correlation energies ($E_{\mathrm{corr},i}(m)$) of all five species as predicted by the ab initio methods. Calculations in each row of the table were performed at the (U)B3LYP optimized geometry of the relevant species. The last column of the table gives the CC values in kcal/mol, which will be used as reference data. As stated before, the three stable species have similar correlation energies, with **bcp** and **tcp** having slightly more (3.7 and 2.25 kcal/mol, respectively) than **cp**. On the average, the CASSCF methods recovered only 9.5 and 16% of the correlation energy with CAS44 and CAS88, respectively. CASSCF-MP2 was much better, the correlation energy recovered reaching about 92%. A serious problem with CASSCF is its uneven recovery of the correlation energy. Thus, even though **cp**, **bcp**, and **tcp** have similar CC correlation energies with the first species having the least amount, CASSCF predicts **cp** to have the largest correlation energy among the three. Consequences of such behavior are quantified in Table 3,[43] which gives the relative correlation energies ($\Delta E_{\mathrm{corr},i}(m)$) in kcal/mol as predicted by all methods considered in this work. It will be observed that the CAS88 predictions for the relative correlation energies in **bcp** and **tcp** are in error by about 12 and 16 kcal/mol, respectively. It should also be noted that the B3LYP and CAS88-MP2 predictions for these two species are in satisfactory agreement with the CC values.

The reaction enthalpies at 298 K calculated by various methods for the rearrangements of **bcp** and **tcp** into **cp** are collected in Tables 4 and 5, respectively, which also include the activation enthalpies to be discussed in the sequel. As stated above, the experimental value for the conversion of **bcp** into **cp** at 25 °C is −47.8 kcal/mol. The predictions by RHF, B3LYP, CC, CAS44-MP2, and CAS88-MP2 methods are within roughly 1.5 kcal/mol of the experimental value, and they all may be considered to be equally good (Table 4). No experimental quantitative data is available for the conversion of **tcp** into **cp**. Assuming that the CC prediction ($\Delta H_r = -63.65$ kcal/mol) is nearest to the actual one, RHF, B3LYP, and CAS88-MP2 perform reasonably well, being within 3 kcal/mol of the CC value, with B3LYP closest to CC (Table 5).

Turning now to the activation enthalpies, for the rearrangement of **bcp** into **cp** (Table 4), the experimental $\Delta H^{\ddagger}$ is 26 kcal/mol. The CC prediction is 25.5 kcal/mol with the UB3LYP and UBPW91 values of 23.6 and 25.2 kcal/mol, respectively, nearly paralleling CC in accuracy, and the CASSCF-MP2 value is 20.2 kcal/mol for both CAS44-MP2 and CAS88-MP2, being about 5 kcal/mol too low relative to CC. The good performance of the broken-symmetry spin-unrestricted DFT in **ts_bcp** comes as a surprise because there is a significant amount of biradical character in this species by all measures mentioned above (vide infra). The vertical S−T gaps in **ts_bcp** as calculated by various methods are given in the first row of Table 6. For the DFT methods, $\langle S^2 \rangle$ values are also shown in parentheses. It should be noted that each method in the table employed its own

TABLE 3: Relative[a] Correlation Energies (kcal/mol) of Various Species at (U)B3LYP/6-31G(d) Optimized Geometries Predicted by Different Methods

	(U)B3LYP	(U)BPW91	CAS44	CAS44-MP2	CAS88	CAS88-MP2	CR-CCSD(T)
bcp	−2.53	−6.14	4.67	−0.17	8.56	−3.58	−3.70
tcp	−2.17	−8.50	12.76	4.69	13.77	0.45	−2.25
ts_bcp	−21.54	−23.93	−25.47	−26.82	−18.62	−29.37	−20.81
ts_tcp	−38.74	−42.96	−31.98	−34.96	−25.96	−38.20	−30.18

[a] $\Delta E_{\mathrm{corr},i}(m)$ relative to **cp**.

TABLE 4: Activation and Reaction Enthalpies (kcal/mol) for the Rearrangement of bcp into cp at 298 K at Different Levels of Theory Using the 6-31G(d) Basis Set

	UB3LYP	UBPW91	RHF[a]	CR-CCSD(T)[a]	CAS44	CAS44-MP2[b]	CAS88	CAS88-MP2[c]	exptl
$\Delta H^{\ddagger}$	23.56	25.22	42.58	25.47	13.32	20.05	16.64	20.18	26[d]
ΔH_r	−47.66	−44.09	−50.19	−46.49	−54.94	−49.73	−58.20	−46.86	−47.8[e]

[a] Calculated at the (U)B3LYP optimized geometries and (U)B3LYP ZPVEs and thermal corrections are used. [b] Calculated at the CAS44 optimized geometries and CAS44 ZPVEs and thermal corrections are used. [c] Calculated at the CAS88 optimized geometries and CAS88 ZPVEs and thermal corrections are used. [d] Reference 1b and c (measurements in the range of 299−381 K). [e] Reference 6 (at 298 K).

TABLE 5: Activation and Reaction Enthalpies (kcal/mol) for the Rearrangement of tcp into cp at 298 K at Different Levels of Theory Using the 6-31G(d) Basis Set

	UB3LYP	UBPW91	RHF[a]	CR-CCSD(T)[a]	CAS44	CAS44-MP2[b]	CAS88	CAS88-MP2[c]
$\Delta H^{\ddagger}$	39.67	42.13	76.25	48.31	33.82	40.47	39.01	40.48
ΔH_r	−63.73	−57.49	−65.90	−63.65	−79.03	−70.80	−79.52	−66.94

[a] Calculated at the (U)B3LYP optimized geometries and (U)B3LYP ZPVEs and thermal corrections are used. [b] Calculated at the CAS44 optimized geometries and CAS44 ZPVEs and thermal corrections are used. [c] Calculated at the CAS88 optimized geometries and CAS88 ZPVEs and thermal corrections are used.

TABLE 6: Vertical Singlet−Triplet Splitting Energies[a] in kcal/mol and Spin Contaminations ($\langle S^2\rangle$ for Singlets in Parentheses) in DFT Methods of the Transition Structures

	UB3LYP[b]	UBPW91[c]	CAS44[d]	CAS44-MP2[d]	CAS88[e]	CAS88-MP2[e]
ts_bcp	10.95 (0.684)	6.94 (0.741)	6.30	4.53	6.24	4.85
ts_tcp	2.65 (0.889)	3.12 (0.935)	−1.49	−3.42	−2.32	−3.02

[a] $\Delta E = E_{\text{triplet}} - E_{\text{singlet}}$, using the 6-31G(d) basis set and not including ZPVEs. [b] Calculated at the UB3LYP optimized singlet geometries. [c] Calculated at the UBPW91 optimized singlet geometries. [d] Calculated at the CAS44 optimized singlet structures. [e] Calculated at the CAS88 optimized singlet structures.

optimized geometry of the singlet biradical at which the S−T gap was computed. All methods predict the ground state of **ts_bcp** to be a singlet. At the UB3LYP geometry, the S−T gap is a small 10.95 kcal/mol with a high spin contamination of $\langle S^2\rangle = 0.68$ in the singlet. The singlet RB3LYP energy at the UB3LYP geometry was calculated to be 5.55 kcal/mol above the spin-unrestricted energy. The biradical character is overestimated by the CASSCF method, as also reflected in its prediction of TS geometry. Thus, referring to Figure 1, one sees that the C1−C4 distance in the CAS88 **ts_bcp** is 0.14 Å longer than that predicted by UB3LYP. More bond breaking at TS is predicted by CASSCF, which in turn implies more localized spins. Because of the longer distance between the radical centers, the spins in the CASSCF TS have a weaker coupling than in UB3LYP, with the result that the S−T gap at the CASSCF geometry is smaller (Table 6).

Nevertheless, the CASSCF calculations provide more insight into why the path between **cp** and **bcp** is W−H forbidden. It suffices to consider CAS44 IRC results for this discussion. Denoting the four π MOs[44] of planar **cp** by π_1, π_2(HOMO), π_3(LUMO), and π_4, the wave function (for the four active electrons) of **cp** is

$$C_1[\pi_1^2\pi_2^2] - C_2[\pi_1^2\pi_3^2]$$

In **cp**, $C_1 > 0.95$ and $C_2 < 0.2$. Along the IRC from **cp** to **ts_bcp**, the original π orbitals continuously distort their shapes with a concomitant change in coefficients C_1 and C_2.[45] Shortly before reaching **ts_bcp**, the second configuration becomes dominant (i.e., $C_2 > C_1$). At the transition structure, $C_1 \approx 0.4$ and $C_2 \approx 0.9$. On continuing the path from **ts_bcp** to **bcp**, the dominance of the second configuration remains intact. Thus, the forbidden nature of the interconversion is due to the abrupt change in the dominant configuration while climbing the barrier from **cp** to **bcp** (on the **cp** side of TS).

Ring opening of the C_{2v}-symmetric **tcp** into the transition structure, **ts_tcp**, takes place in the following manner. (See Figure 1 and the numbering in Scheme 1.) One of the two equivalent carbons at positions 1 or 4 rotates around the C_2 axis. Taking C4 as the moving carbon (together with its hydrogen), its rotation continues until it becomes approximately coplanar with C1, C3, and C5. In the meantime, C2 rotates around the C1−C3 bond outward so that the C2−C3−C1−C5 torsion angle increases by 21.2° at the UB3LYP level (23.8° at CAS88) when **ts_tcp** is reached. The net effect is the breakage of the C2−C4 bond while the length of the C1−C3 bond increases by a minor 0.05 Å (0.1 Å at CAS88). The C1−C3 bond is broken on the **cp** side of the reaction path, accompanied by the formation of the two π bonds.

Assessing the performance of various methods in predicting the relative energy of **ts_tcp** is not easy. The UDFT methods predict geometries at which the ground state is a singlet whereas CASSCF predicts just the opposite (Table 6). The PESs belonging to the two spin states are nearly degenerate in the vicinity of **ts_tcp**, and it is certain that they cross between the UDFT and CASSCF structures (Figure 2). Indeed, the UB3LYP

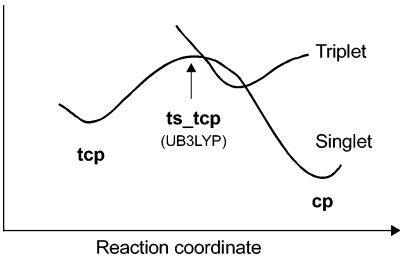

Figure 2. Qualitative behavior of the minimum energy path in the isomerization of **tcp**, showing the intersystem crossing.

IRC quickly crosses into the triplet surface at a reaction coordinate (rxc) value of 0.4 amu$^{1/2}$•bohr on the **cp** side of the TS and crosses out of it at rxc = 1.7 amu$^{1/2}$•bohr. The minimum of the nearby triplet surface[41] is calculated to be about 3 kcal/mol below the singlet saddle point at both the UB3LYP and CAS88-MP2 levels. The structure of the molecule at the triplet minimum is quite similar to **ts_tcp**. At the singlet UB3LYP saddle point where the triplet lies higher in energy, the S−T gap is calculated to be 2.65 and 3.79 kcal/mol by the UB3LYP and CAS88-MP2 methods, respectively. The latter value should be more trustworthy because CASSCF-MP2 preserves the spin symmetry. As expected, the spin contamination, $\langle S^2\rangle = 0.89$, in UB3LYP is higher than that in **ts_bcp**.

The heats of formation of **ts_tcp** relative to those of **tcp** (i.e., the activation enthalpy) calculated at different levels of theory are given in the first row of Table 5. The lack of experimental data makes it difficult to judge the reliability of these values. The UB3LYP and CASSCF-MP2 predictions are in close agreement with each other, and the UBPW91 estimate is within 2 kcal/mol of the former values. Shall we trust the UB3LYP result, especially considering its unexpected success in the case of **ts_bcp**? The answer appears to be no. Reference to Table 1 shows that the agreement among UB3LYP, UBPW91, and CASSCF-MP2 is due to fortuitous cancellations. Although the success of computational chemistry is largely dependent on the systematic cancellation of errors, there are inconsistencies in our case. The high-level CC calculations employing the same geometries as in UB3LYP predict an activation enthalpy that is 8 kcal/mol higher. Of course it is possible that the CC calculations are in error because the CR-CCSD(T) method we used is based on the RHF determinant and hence it may be unable to handle the multireference nature of the wave function in **ts_tcp**. However, the TS under consideration effectively contains one broken bond, and as mentioned before, CR-CCSD(T) has been shown to be successful even in the case of two broken bonds. Further evidence supporting CC comes from the data in Tables 2 and 3. It is seen from Table 3 that the CAS88-MP2 method overestimates the correlation energy of **ts_bcp** relative to that in **cp** by 8.5 kcal/mol. At this geometry, the CR-CCSD(T) method (also UB3LYP) works excellently. Assuming that CAS88-MP2 overestimates the relative correlation energy of the **ts_tcp** structure by the same amount, an assumption supported by the data in Table 2 (93.7% recovery in both TSs), we conclude that the CC results are probably

TABLE 7: CAS88[a] Mulliken Effectively Unpaired Electron Populations and Biradical Indices[b,c]

	cp	bcp	tcp	ts_bcp	ts_tcp
C1	0.18 (0.19)	0.10 (0.11)	0.10 (0.11)	0.57 (0.80)	0.13 (0.16)
C2	0.17 (0.18)	0.21 (0.22)	0.11 (0.12)	0.23 (0.27)	0.80 (0.94)
C3	0.17 (0.18)	0.21 (0.22)	0.11 (0.12)	0.23 (0.27)	0.11 (0.16)
C4	0.18 (0.19)	0.10 (0.11)	0.10 (0.11)	0.57 (0.80)	0.82 (0.98)
C5	0.00 (0.00)	0.00 (0.00)	0.00 (0.00)	0.02 (0.02)	0.00 (0.01)
br	0.06 (0.10)	0.03 (0.09)	0.02 (0.04)	0.34 (0.59)	0.56 (0.98)

[a] 6-31G(d) basis set. See Scheme 1 for the numbering of carbon atoms. [b] In each pair of numbers in the Table, the first one refers to the spin population calculated at the UB3LYP optimized geometry, and the second one, shown in parentheses, is the corresponding value at the CAS88 optimized geometry. [c] For comparison, the net spin population on each carbon in benzene is 0.16, and br = 0.10 (with CAS66 employing the 6 π MOs).

correct and that the UB3LYP method is also suffering from the overestimation problem.

If the energies of **ts_tcp** predicted by UB3LYP and CASSCF are both unreliable, then what is the correct geometry of this TS? The CR-CCSD(T) energy of the UB3LYP optimized structure differs significantly from the corresponding CC energy of the CAS88 optimized structure; the UB3LYP **ts_tcp** was lower in energy by 11.80 kcal/mol. (The analogous difference in **ts_bcp** was 7.04 kcal/mol.[46]) There are indications that the UB3LYP geometry is more plausible. The distance between C2 and C4 (one of the two broken bonds) is 2.30 Å in the product, **cp** (Figure 1). In the TS, according to UB3LYP, the breakup of this bond is completed (C2−C4 = 2.31 Å in **ts_tcp**) whereas CAS88 predicts it to be 0.14 Å longer. This behavior of CASSCF, predicting the length of a breaking bond exceeding its ultimate value at some intermediate point along the reaction path, is not sensible on chemical grounds. It appears that the UB3LYP structure should be closer to the actual one. Our estimate of the activation enthalpy in the rearrangement, **tcp** to **cp**, is then ~48 kcal/mol at the CR-CCSD(T) level of theory (Table 5).[47]

Biradical Character. To account for the presence of unpaired electrons in singlet biradicals, a density-like function has been proposed in ref 37.

$$D(\mathbf{r}) = 2\rho(\mathbf{r}) - \int \rho(\mathbf{r}|\mathbf{r}')\,\rho(\mathbf{r}'|\mathbf{r})\,\mathrm{d}\mathbf{r}'$$

where $\rho(\mathbf{r}|\mathbf{r}')$ is the one-electron spin-free reduced density matrix. Termed[37c] as the "density of effectively unpaired electrons", the function $D(\mathbf{r})$ describes the spatial separation of α and β electrons. Table 7 lists the Mulliken atomic populations of $D(\mathbf{r})$ calculated with CAS88 wave functions for the five species considered in this work.

It should be noted that when calculated with correlated wave functions the density $D(\mathbf{r})$ gives rise to a partial splitting of electron pairs even in closed-shell molecules.[37e,f] For example, in the **tcp** molecule, consisting of single C−C bonds, there is roughly 0.1 unpaired electron on each of the C1, C2, C3, and C4 atoms (Table 7). The prediction of no free spin on C5 is actually spurious and is due to the limitations of the active space employed; our (8e, 8o) active space did not correlate the electrons in the C5−C1 and C5−C4 bonds. The more extensive (12e, 12o) active space would probably assign a similar 0.1 unpaired electron on C5 as well. Note also that the amount of free spin on such carbon atoms in the other molecules in Table 7 is nearly the same (C1, C4 in **bcp**; C1, C3 in **ts_tcp**). Carbons involved in π bonds have larger (0.17−0.23) free spins (C1••C4 in **cp**; C2, C3 in **bcp** and **ts_bcp**). Similar values were obtained in other π systems. For example, CASSCF/6-31G(d) calculations on ethylene and benzene yielded 0.16−0.17 unpaired electron on each carbon atom.

Referring to the **ts_bcp** and **ts_tcp** columns of Table 7, there is a marked accumulation of unpaired electrons on the carbon atoms of the cleaving bond. The number of free spins predicted on each carbon of the breaking bond is 0.57 (0.80) and 0.81 (0.96)[48] at the UB3LYP (CAS88) geometries in **ts_bcp and ts_tcp**, respectively. These results unequivocally verify the expected biradical character of these transition structures. Using Jensen's br, the biradical character in **ts_bcp** and **ts_tcp** is 34% (59%) and 56% (98%), respectively, at the UB3LYP (CAS88) geometries. The larger values predicted by CASSCF for both the biradical indices and the number of unpaired electrons are clearly due to the longer distances between the radical centers at the CASSCF optimized geometries (Figure 1).

We next demonstrate that the biradical character in **ts_bcp** and **ts_tcp** can be rationalized almost quantitatively by just considering the frontier natural orbitals (NO). Using natural orbitals, the density $D(\mathbf{r})$ has the form[37c]

$$D(\mathbf{r}) = \sum n_k(2 - n_k)\,\varphi_k(\mathbf{r})^2$$

where $\varphi_k(\mathbf{r})$ is a NO and n_k is its occupation number.[49] Generally, this is a convenient expression in CASSCF calculations because the number of nonzero terms in the sum cannot exceed the number of active orbitals employed (i.e., $n_k = 2$ for the occupied orbitals not included in the active space). For a system with $2N$ electrons, the most important contributions are made by NOs corresponding to the HOMO and LUMO. Setting $h = N$ and $l = N + 1$, we denote these NOs by φ_h and φ_l, respectively. Furthermore, our calculations indicate that $n_h + n_l \approx 2$,[50] so the contribution from the HOMO−LUMO pair becomes

$$d(\mathbf{r}) \equiv n_h n_l(\varphi_h(\mathbf{r})^2 + \varphi_l(\mathbf{r})^2)$$

The CAS88 orbitals φ_h and φ_l in the transition structures **ts_bcp** and **ts_tcp** are displayed in Figure 3; it is seen that they extend over both radical centers. Defining (pseudo)localized orbitals by

$$\varphi_R = \frac{(\varphi_h + \varphi_l)}{\sqrt{2}}$$

$$\varphi_S = \frac{(\varphi_h - \varphi_l)}{\sqrt{2}}$$

we express the density $d(\mathbf{r})$ equivalently as

$$d(\mathbf{r}) = n_h n_l(\varphi_R^2 + \varphi_S^2)$$

As intentionally emphasized in Figure 3, these orbitals are sufficiently concentrated on each radical center, allowing us to interpret $n_h n_l$ as the number of unpaired spins on each carbon of the cleaving bond. The CAS88 values of n_h at the UB3LYP (CAS88) geometries are 1.66 (1.41) and 1.44 (1.02) for **ts_bcp** and **ts_tcp**, respectively, yielding 0.56 (0.83) and 0.81 (1.00) for $n_h n_l$ in the two systems. The agreement between the simplified picture and the full calculation (Table 7) is impressive.

It is tempting to apply these ideas to the broken-symmetry UB3LYP determinant. Distinguishing the UB3LYP NOs and their occupation numbers by the superscript u, it may be shown[37c] that for a singlet state $\Sigma n_k^{\mathrm{u}}(2 - n_k^{\mathrm{u}}) = 2\langle S^2\rangle$, giving the total number of effectively unpaired electrons as twice the spin contamination. Unlike CASSCF, all occupation numbers

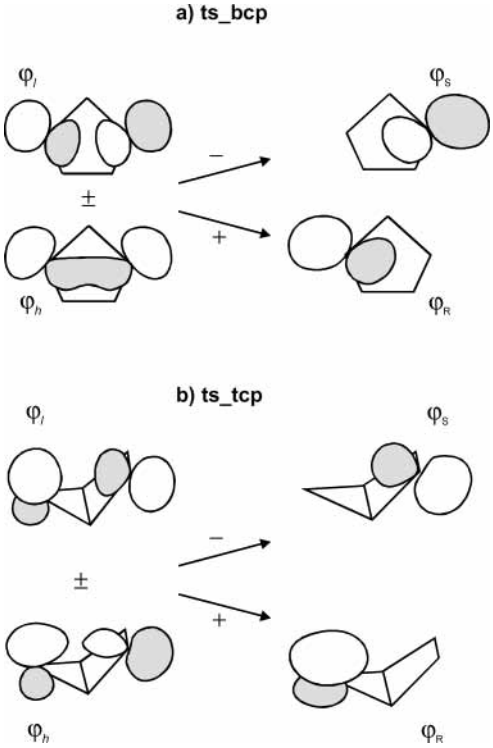

Figure 3. CAS88 frontier natural orbitals (left) and localized radical orbitals (right) of **ts_bcp** and **ts_tcp**.

of UB3LYP NOs are nearly 2 (or 0) in both **ts_bcp** and **ts_tcp**, except for the HOMO−LUMO pair. Hence,[50] $n_h^u(2 - n_h^u) = n_h^u n_l^u \approx \langle S^2 \rangle$. The values of n_h^u are 1.58 and 1.34 in **ts_bcp** and **ts_tcp**, respectively, yielding 0.664 and 0.884 for the product $n_h^u n_l^u$ in the two systems as compared with the accurate values 0.684 and 0.889 for $\langle S^2 \rangle$ (Table 6). The corresponding UB3LYP NOs[51] φ_h^u and φ_l^u are similar to the CASSCF NOs shown in Figure 3, except for some contribution from the p orbitals on C2 and C3 in the case of **ts_bcp**. In summary, assuming that it is permissible to use the UB3LYP determinant for the analysis of $D(\mathbf{r})$, the spin contamination $\langle S^2 \rangle$ in singlet biradicals may be interpreted as the number of effectively free spins on each radical center. In any case, it is interesting that there is considerable overlap between CASSCF and UB3LYP results regarding the distribution of effectively unpaired electrons.

Conclusions

The reaction paths in the ring opening of two strained isomers of cyclopentadiene were studied by a combination of density functional theory and high-level ab initio methods. Both processes are concerted, and the paths pass through transition states with a high degree of biradical character. In both reactions, the π bonds of cyclopentadiene are formed after the TSs, on the **cp** side of the paths. Geometries at the potential energy minima predicted by the DFT and CASSCF methods were equally good. We found that CC and B3LYP methods predicted the reaction enthalpies excellently (−47.7 vs expt[6] = −47.8 kcal/mol for **bcp** and −63.7 kcal/mol for **tcp** at the B3LYP level) whereas the MCSCF method did not perform as well. The expensive CAS88 calculations gave reaction energies that were in error by 10 kcal/mol for **bcp** and 13 kcal/mol for **tcp**, which were improved when dynamic correlation energy was taken into account. The activation enthalpy for the ring opening of **bcp** was calculated by the CR-CCSD(T) method to be 25.5 kcal/mol, in good agreement with experiment. The value obtained by the UB3LYP method was a satisfactory 23.6 kcal/mol even though there was high spin contamination ($\langle S^2 \rangle$ = 0.68) in the singlet biradical transition state. It appears that the B3LYP functional is quite resistant to the possible consequences of spin contamination. The performance of CAS88-MP2 was poorer, predicting the activation enthalpy to be too low by 6 kcal/mol. The low activation energies given by CASSCF-MP2 were rationalized by showing that the method overestimated the correlation energy of biradical structures, a problem shared by UB3LYP when spin contamination is too high. CASSCF also overestimated the biradical character by predicting unrealistically long distances between the radical centers. The transition structure, **ts_tcp**, was found to be nearly degenerate with the triplet state, making the reliable assessment of its properties very difficult.[52] We argued that the energy obtained by the UB3LYP method for this structure was probably too low, as in CAS88-MP2, but that the geometry was more plausible than that predicted by the CAS88 method. Using the UB3LYP structure, the activation enthalpy for the ring opening of **tcp** was obtained by the CR-CCSD(T) method to be 48.3 kcal/mol.

Measures of biradical character in the transition states by $\langle S^2 \rangle$, the vertical S−T gap, the biradical index, and through an analysis of the density of effectively unpaired electrons were in qualitative agreement with each other. In particular, we found that the distribution of free spins in both **ts_bcp** and **ts_tcp** could be predicted by a consideration of frontier natural orbitals only.

Supporting Information Available: Energies (hartree), geometries, vibrational frequencies, and zero-point vibrational energies of all stationary structures shown in Figure 1 at the (U)B3LYP, (U)BPW91, CAS44, and CAS88 levels. This material is available free of charge via the Internet at http://pubs.acs.org.

References and Notes

(1) (a) Brauman, J. I.; Ellis, L. E.; Tamelen, E. E. *J. Am. Chem. Soc*. **1966**, *88*, 846. (b) Brauman, J. I.; Golden, D. M. *J. Am. Chem. Soc*. **1968**, *90*, 1920. (c) Golden, D. M.; Brauman, J. I. *Trans. Faraday Soc*. **1969**, *65*, 464.

(2) (a) Baldwin, J. E.; Pinschmidt, R. K. *J. Am. Chem. Soc*. **1970**, *92*, 5247. (b) Baldwin, J. E.; Pinschmidt, R. K.; Andrist, A. H. *J. Am. Chem. Soc*. **1970**, *92*, 5249. (c) Hsu, S. L.; Andrist, A. H.; Gierke, T. D.; Benson, R. C.; Flygare, W. H.; Baldwin, J. E. *J. Am. Chem. Soc*. **1970**, *92*, 5250. (d) Andrews, G. D.; Baldwin, J. E. *J. Am. Chem. Soc*. **1977**, *99*, 4851. (e) Andrews, G. D.; Baldwin, J. E. *J. Am. Chem. Soc*. **1977**, *99*, 4853. (f) Andrews, G. D.; Baldwin, J. E.; Gilbert, K. E. *J. Org. Chem*. **1980**, *45*, 1523.

(3) Woodward, R. B.; Hoffmann, R. *Angew*. Chem., Int. Ed. Engl. **1969**, *8*, 781.

(4) For a review of the controversy, see Gajewski, J. J. *Hydrocarbon Thermal Isomerizations*; Academic Press: New York, 1981; pp 75−77.

(5) Altmann, J. A.; Tee, O. S.; Yates, K. *J. Am. Chem. Soc*. **1976**, *98*, 7132.

(6) (a) Roth, W. R.; Klerner, F. G.; Lennartz, H. W. *Chem. Ber*. **1980**, *113*, 1818. (b) Roth, W. R.; Rekowski, V.; Börner, S.; Quast, M. *Liebigs Ann*. **1996**, *3*, 409.

(7) Dewar, M. J. S.; Kirschner, S. *J. Chem. Soc., Chem. Commun*. **1975**, 461.

(8) (a) Bofill, J. M.; Gomez, J.; Olivella, S. *J. Mol. Struct.:* THEOCHEM **1988**, *163*, 285. (b) Olivella, S.; Salvador, J. *J.* Comput. Chem. **1991**, *12*, 792.

(9) Skancke, P. N.; Yamashita, K.; Morokuma, K. *J. Am. Chem. Soc*. **1987**, *109*, 4157.

(10) Jensen, F. *J. Am. Chem. Soc*. **1989**, *111*, 4643.

(11) Hosokawa, T.; Morinati, I. *J. Chem. Soc., Chem. Commun*. **1970**, 905.

(12) Zeller, K. P. *Angew. Chem., Int. Ed. Engl*. **1982**, *21*, 440.

(13) (a) Dowd, P.; Irngartinger, H. *Chem. Rev*. **1989**, *89*, 985. (b) Dowd, P.; Garner, P.; Schappert, R. *J. Org. Chem*. **1982**, *47*, 4240. (c) Dowd, P.; Schappert, R.; Garner, P.; Go C. L. *J. Org. Chem*. **1985**, *50*, 44. (d) Dowd, P.; Schappert, R.; Garner, P. *Tetrahedron Lett*. **1982**, *23*, 3.

(14) Levin, M. D.; Kaszynski, P.; Michl, J. *Chem. Rev*. **2000**, *100*, 169.
(15) Irngartinger, H.; Jahn, R.; Rodewald, H. *J. Am. Chem. Soc*. **1987**, *109*, 6547.
(16) Gleiter, R.; Haider, R.; Bischof, P. *J. Org. Chem*. **1984**, *49*, 375.
(17) Ona, H.; Yamaguchi, H.; Masamune, S. *J. Am. Chem. Soc*. **1970**, *92*, 7495.
(18) Pomerantz, M.; Wilke, R. N. *Tetrahedron Lett*. **1969**, *10*, 463.
(19) Hariharan, P. C.; Pople, J. A. *Theor. Chim. Acta*. **1973**, *28*, 213.
(20) Hehre, W. J.; Ditchfield, R.; Pople, J. A. *J. Chem. Phys*. **1972**, *56*, 2257.
(21) Becke, A. D. *J. Chem. Phys*. **1993**, *98*, 5648.
(22) Lee, C.; Yang, W.; Parr, R. G. *Phys. Rev. B* **1988**, *37*, 785.
(23) (a) Perdew, J. P.; Chevary, J. A.; Vosko, S. H.; Jackson, K. A.; Pederson, M. R.; Singh, D. J.; Fiolhais, C. *Phys. Rev. B* **1992**, *46*, 6671. (b) Perdew, J. P.; Burke, K.; Wang, Y. *Phys. Rev. B* **1996**, *54*, 16533.
(24) Frisch, M. J.; Trucks, G. W.; Schlegel, H. B.; Scuseria, G. E.; Robb, M. A.; Cheeseman, J. R.; Zakrzewski, V. G.; Montgomery, J. A., Jr.; Stratmann, R. E.; Burant, J. C.; Dapprich, S.; Millam, J. M.; Daniels, A. D.; Kudin, K. N.; Strain, M. C.; Farkas, O.; Tomasi, J.; Barone, V.; Cossi, M.; Cammi, R.; Mennucci, B.; Pomelli, C.; Adamo, C.; Clifford, S.; Ochterski, J.; Petersson, G. A.; Ayala, P. Y.; Cui, Q.; Morokuma, K.; Malick, D. K.; Rabuck, A. D.; Raghavachari, K.; Foresman, J. B.; Cioslowski, J.; Ortiz, J. V.; Stefanov, B. B.; Liu, G.; Liashenko, A.; Piskorz, P.; Komaromi, I.; Gomperts, R.; Martin, R. L.; Fox, D. J.; Keith, T.; Al-Laham, M. A.; Peng, C. Y.; Nanayakkara, A.; Gonzalez, C.; Challacombe, M.; Gill, P. M. W.; Johnson, B. G.; Chen, W.; Wong, M. W.; Andres, J. L.; Head-Gordon, M.; Replogle, E. S.; Pople, J. A. *Gaussian 98*, revision A.9; Gaussian, Inc.: Pittsburgh, PA, 1998.
(25) (a) Goldstein, E.; Beno, B.; Houk, K. N. *J. Am. Chem. Soc*. **1996**, *118*, 6036. (b) Houk, K. N.; Beno, B. R.; Nendel, M.; Black, K.; Yoo, H. Y.; Wilsey, S.; Lee, J. K. *J. Mol. Struct.: THEOCHEM* **1997**, *398*−*399*, 169. (c) Hrovat, D. A.; Beno, B. R.; Lange, H.; Yoo, H. Y.; Houk, K. N.; Borden, W. T. *J. Am. Chem. Soc.* **2000**, *122*, 7456.
(26) (a) Staroverov, V. N.; Davidson, E. R. *J. Am. Chem. Soc*. **2000**, *122*, 7377. (b) Staroverov, V. N.; Davidson, E. R. *J. Mol. Struct.: THEOCHEM* **2001**, *573*, 81.
(27) Doering, W. v.; Wang, Y. *J. Am. Chem. Soc*. **1999**, *121*, 10112.
(28) Schmidt, M. W.; Baldridge, K. K.; Boatz, J. A.; Elbert, S. T.; Gordon, M. S.; Jensen, J. H.; Koseki, S.; Matsunaga, N.; Nguyen, K. A.; Su, S.; Windus, T. L.; Dupuis, M.; Montgomery, J. A. *J. Comput. Chem*. **1993**, *14*, 1347.
(29) (a) Ishida, K.; Morokuma, K.; Komornicki, A. *J. Chem. Phys.* **1977**, *66*, 2153. (b) Fukui, K. *Acc. Chem. Res.* **1981**, *14*, 363.
(30) (a) Nakano, H. *J. Chem. Phys*. **1993**, *99*, 7983. (b) Hirao, K. *Chem. Phys. Lett*. **1993**, *201*, 59.
(31) Özkan, I. 2001 (unpublished). In our laboratory, we have developed a graphical interface program that allows the full integration of various packages including Gaussian 98, GAMESS, and HONDO. Hessians, MOs, and geometries as obtained using one program are easily transferable to the others.
(32) (a) Kowalski, K.; Piecuch, P. *Chem. Phys. Lett*. **2001**, *344*, 165. (b) Kowalski, K.; Piecuch, P. *J. Chem. Phys*. **2000**, *113*, 18.
(33) Piecuch, P.; Kucharski, S. A.; Kowalski, K.; Musial, M. *Comput. Phys. Comm*. **2002**, *149*, 71.
(34) For example, CR-CCSD(T) with a double-ζ (DZ) plus polarization basis set calculations for the BH molecule reported in ref 32a showed that the maximum deviation from the full configuration interaction (FCI) value was only 1.1 kcal/mol, even for a 300% stretched B−H bond length. Similarly, using a DZ basis in the water molecule (see ref 32b), the maximum deviation from FCI was 1.6 kcal/mol when the two O−H bonds were simultaneously stretched as much as 200%. These examples correspond to the homolytic cleavage of one and two bonds, respectively, both generating radical systems. Interestingly, in both molecules the CR-CCSD-(T) values were uniformly above the corresponding FCI results, indicating that errors in energies relative to the PES minima are even smaller.
(35) Minkin, V. I. *Pure Appl. Chem*. **1999**, *71*, 1919
(36) Sperling, D.; Fabian, J. *Eur. J. Org. Chem*. **1999**, *215*.
(37) (a) Takatsuka, K.; Fueno, T.; Yamaguchi, K. *Theor. Chim. Acta* **1978**, *48*, 175. (b) Takatsuka, K.; Fueno, T. *J. Chem. Phys.* **1978**, *69*, 661 (c) Staroverov, V. N.; Davidson, E. R. *Chem. Phys. Lett*. **2000**, *330*, 161. (d) Staroverov, V. N.; Davidson, E. R. *J. Am. Chem. Soc*. **2000**, *122*, 186. (e) Lain, L.; Torre, A.; Bochicchio, R. C.; Ponec, R. *Chem. Phys. Lett*. **2001**, *346*, 283. (f) Torre, A.; Lain, L.; Bochicchio, R. *J. Phys. Chem. A* **2003**, *107*, 127.
(38) (a) Mayer, I. *Int. J. Quantum Chem*. **1986**, *29*, 73. (b) Mayer, I. *Int. J. Quantum Chem*. **1986**, *29*, 477. (c) Villar, H. O.; Dupuis, M. *Chem. Phys. Lett*. **1987**, *142*, 59.
(39) Dupuis, M.; Marquez, A.; Davidson, E. R. *HONDO 8.5*; IBM Corp.: Kingston, NY, 1994.
(40) Krishnan, R.; Binkly, J. S.; Seeger, R.; Pople, J. A. *J. Chem. Phys*. **1980**, *72*, 650.
(41) Energies, geometries, vibrational frequencies, and ZPVEs of all species at the (U)B3LYP, (U)BPW91, CAS44, and CAS88 levels are available in the Supporting Information, which also includes the UB3LYP and CAS88 optimized triplet minimum structures close to **ts_tcp**.
(42) Damiani, D.; Ferreti, L.; Gallinella, E. *Chem. Phys. Lett*. **1976**, *37*, 265.
(43) CASSCF and CASSCF-MP2 values in Table 3 can be obtained from the data of Table 2.
(44) In point groups C_{2v}(C_s) of the planar **cp** (intermediate structures), these orbitals have the symmetry species $b_1(a')$, $a_2(a'')$, $b_1(a')$, and $a_2(a'')$, in order.
(45) Coefficients C_1 and C_2 refer to the CASSCF wave function constructed using the natural orbitals.
(46) The UB3LYP and CAS88 optimized structures have very similar UB3LYP energies in both TSs. The difference, E(UB3LYP//CAS88) − E(UB3LYP//UB3LYP), is only +0.14 and −0.40 kcal/mol for **ts_tcp** and **ts_bcp**, respectively.
(47) It may be of interest to note that the standard CCSD(T) estimates of activation energies are too low (relative to CR-CCSD(T)) by 2.68 and 5.53 kcal/mol for **ts_bcp** and **ts_tcp**, respectively.
(48) Average of values for the two carbons in the breaking bond.
(49) We assume that the NOs have been ordered such that $n_{k+1} < n_k$ for $k = 1, 2,...$
(50) This property holds (approximately) for all CASSCF NO pairs in the systems studied here. Note also that it is an exact relationship for the NOs of UHF or UDFT wave functions; see, for example, ref 37c.
(51) Note that whereas the UB3LYP MOs are not symmetrical all NOs are symmetry orbitals.
(52) Near degeneracy of the singlet and triplet surfaces enhances spin contamination in DFT-based methods, raising doubts about their predictions. Similarly, CASSCF does not seem to have sufficient accuracy in predicting a reliable geometry under the same conditions.